Structural and magnetic characterization of the intermartensitic phase transition in NiMnSn Heusler alloy ribbons

J. L. Sánchez Llamazares, H. Flores-Zúñiga, D. Ríos-Jara, C. F. Sánchez-Valdes, T. García-Fernández, C. A. Ross, and C. García

Citation: Journal of Applied Physics **113**, 17A948 (2013);
View online: https://doi.org/10.1063/1.4800836
View Table of Contents: http://aip.scitation.org/toc/jap/113/17
Published by the American Institute of Physics

Structural and magnetic characterization of the intermartensitic phase transition in NiMnSn Heusler alloy ribbons

J. L. Sánchez Llamazares,[1,a)] H. Flores-Zúñiga,[1] D. Ríos-Jara,[1] C. F. Sánchez-Valdes,[2] T. García-Fernández,[3] C. A. Ross,[4] and C. García[4,5,6]
[1]*Instituto Potosino de Investigación Científica y Tecnológica A.C., Camino a la Presa San José 2055 Col. Lomas 4a, San Luis Potosí S.L.P. 78216, Mexico*
[2]*Institut de Ciencia de Materials de Barcelona, CSIC, Campus UAB, 08193 Bellaterra, Spain*
[3]*Universidad Autónoma de la Ciudad de México, Prolongación San Isidro 151, Col. San Lorenzo Tezonco, México DF C.P. 09790, Mexico*
[4]*Department of Materials Science and Engineering, Massachusetts Institute of Technology, Cambridge, Massachusetts 02139, USA*
[5]*Physics Department, Bogaziçi University, North Campus KB 331-O, Bebek/Istanbul, Turkey*
[6]*Departamento de Fisica, Universidad Técnica Federico Santa María, P.O. Box 110-V, Valparaiso, Chile*

(Presented 16 January 2013; received 10 November 2012; accepted 29 January 2013; published online 3 May 2013)

Phase transitions and structural and magnetic properties of rapidly solidified $Ni_{50}Mn_{38}Sn_{12}$ alloy ribbons have been studied. Ribbon samples crystallize as a single-phase, ten-layered modulated (10M) monoclinic martensite with a columnar-grain microstructure and a magnetic transition temperature of 308 K. By decreasing the temperature, martensite undergoes an intermartensitic phase transition around 195 K. Above room temperature, the high temperature martensite transforms into austenite. Below 100 K, magnetization hysteresis loops shift along the negative H-axis direction, confirming the occurrence of an exchange bias effect. On heating, the thermal dependence of the coercive field H_C shows a continuous increase, reaching a maximum value of 1017 Oe around 50 K. Above this temperature, H_C declines to zero around 195 K. But above this temperature, it increases again up to 20 Oe falling to zero close to 308 K. The coercivity values measured in both temperature intervals suggest a significant difference in the magnetocrystalline anisotropy of the two martensite phases. © *2013 AIP Publishing LLC*. [http://dx.doi.org/10.1063/1.4800836]

The study of structural and magnetic transitions in the off-stoichiometric Heusler-based system $Ni_{50}Mn_{50-x}Sn_x$ has drawn considerable attention in the last few years.[1] In the critical composition range of $13 \leq x \leq 15$, these alloys undergo a first-order martensitic transformation (MT) from a cubic austenite (AST) to a structurally modulated martensite (MST), in which both phases exhibit dominant ferromagnetic (FM) ordering,[2–4] although MT is observed in the concentration range $5 \leq x \leq 25$.[3]

In addition to the MT an intermartensitic transformation may also exist in alloys undergoing a first-order MT. The intermartensitic transformation is a phase transformation between martensites with different structures that takes place upon cooling at temperatures below the martensitic final M_f phase transition temperature.[5,6] Several intermartensitic transitions have been reported so far in different alloy systems such as TiNiCu alloys,[7,8] $Ni_{64}Al_{34.5}Re_{1.5}$,[9] NiAlMn,[10,11] NiMnGa alloys,[12–17] NiFeGa,[18] and NiMnInSb,[19] among others.

Rapid solidification by using the melt-spinning technique is an effective one-step process to obtain single phase alloy ribbons in the $Ni_{50}Mn_{50-x}Sn_x$ system.[20–22] When these alloys are produced by means of this technique, the microstructure is considerably refined in average grain size and shows lower martensitic starting temperature M_S in comparison with bulk alloys with similar composition.[2,3,23] From the study of a series of as-quenched (aq) $Ni_{50}Mn_{50-x}Sn_x$ ($12 \leq x \leq 15$) melt spun alloys, an intermartensitic phase transition has been observed in samples of nominal composition $Ni_{50}Mn_{38}Sn_{12}$. Herein, we present the structural and magnetic characterizations of this alloy in which the phase transitions have been studied by thermomagnetic measurements and differential scanning calorimetry (DSC). As described below, the results are different from those reported for bulk alloys with similar valence electron concentration per atom (e/a) ratio.[3]

Alloy ribbons were fabricated from arc melted bulk ingots of nominal composition $Ni_{50}Mn_{38}Sn_{12}$ (<0.1 % at.) in a high purity Ar atmosphere at a linear speed of the copper wheel of 48 ms^{-1}. Phase identification was made from X-ray diffraction (XRD) patterns of powdered samples. XRD patterns were measured using a Bruker D8 Advance diffractometer (Cu-Kα radiation). DSC curves were measured with a TA Instruments model 200 calorimeter with a heating/cooling rate of 5 K/min. Magnetization (M) measurements were made by means of a physical properties measurement system (Quantum Design PPMS® EverCool, 90 kOe) using the vibrating sample magnetometer module. The magnetic field H was applied along the ribbon axis (i.e., rolling direction) to minimize the demagnetizing field effect.

The ribbon flakes obtained were fully crystalline with the following physical dimensions: 7–10 μm in thickness, 1.5–2.0 mm in width, and 5–12 mm in length. The homogeneous composition of chemical elements and the single-phase character of the ribbons were confirmed by scanning electron

a)Author to whom correspondence should be addressed. Electronic mail: jose.sanchez@ipicyt.edu.mx

microscopy (SEM) examinations in the backscattered electron emission mode. The average chemical composition, determined by energy dispersive spectroscopy (EDS) from numerous analyses performed on both sample cross-sections and ribbon surfaces for different ribbon flakes, was $Ni_{51.2}Mn_{36.8}Sn_{12.0}$. Hence, the aq alloy ribbons show a higher Ni/Mn ratio than that of the nominal composition and therefore their e/a is 8.18.

The left column of Fig. 1(a) shows the SEM images of the typical microstructure of the ribbons studied. Ribbons show a highly oriented columnar-grain microstructure in which the longer axis of individual grains is oriented perpendicular to both ribbon surfaces. A higher resolution SEM micrograph of the free-surface of ribbons is presented on the right side of Fig. 1(a). It clearly shows the characteristic elongated thin plates, or strips, corresponding to MST variants. The room-temperature XRD powder pattern is shown in Fig. 1(b). All of the XRD reflections have been satisfactorily indexed as corresponding to a ten-layered modulated (10M) monoclinic structure with cell parameters $a = 0.4196$ nm, $b = 0.5647$ nm, $c = 2.145$ nm, and $\beta = 88.08°$. Hence, the SEM observations and XRD analysis indicate that MST is the existing phase at room temperature.

Figure 2(a) shows the temperature dependencies of magnetization *M(T)* measured in zero-field cooled (ZFC), field-cooled (FC), and field-heated (FH) regimes at $H = 50$ Oe and $H = 50$ kOe, respectively. The arrows in this figure indicate whether the curve pathway corresponds to a heating or a cooling regime, as well as the scale of each curve. The room temperature 10M MST exhibits a magnetic ordering temperature of 308 K. Upon cooling, a major magnetic transition occurs at 195 K. Below this temperature, the FC and FH pathways of the low-field *M(T)* curve split with respect to the ZFC pathway indicating that the sample is magnetically inhomogeneous. From earlier studies with this type of ferromagnetic shape memory alloys, this behavior has been attributed to the coexistence of

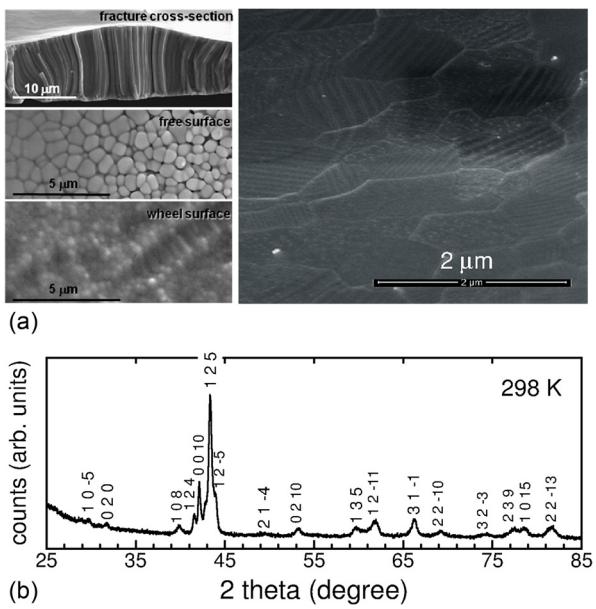

FIG. 1. (a) Typical microstructure of $Ni_{50}Mn_{38}Sn_{12}$ alloy ribbons. Left images: fracture cross-section (top), ribbon free-surface (middle), and ribbon wheel-side ribbon surface (bottom). Right image: free surface of ribbons showing the characteristic twinned microstructure of MST. (b) XRD pattern at 298 K for aq $Ni_{50}Mn_{38}Sn_{12}$ ribbons, indexed as shown by the indices hkl.

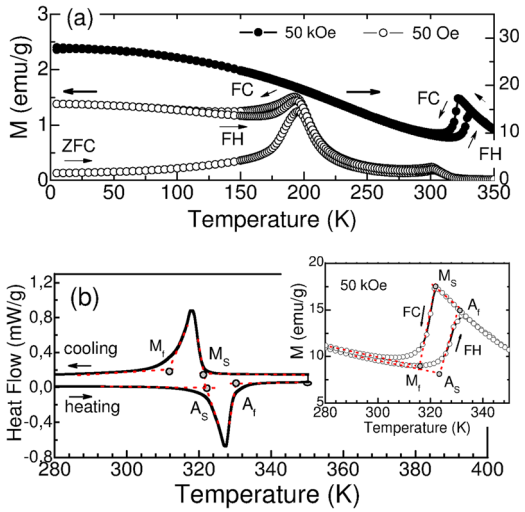

FIG. 2. (a) ZFC, FC, and FC *M(T)* curves at 50 Oe and 50 kOe. (b) DSC scans in the temperature range in which the room temperature MST transforms into a nonmagnetic AST. Inset: FH and FC *M(T)* curves measured under $H = 50$ kOe. The extrapolation method used to determine the structural transition temperatures is illustrated in both graphs.

antiferromagnetic (AFM) and FM exchange interactions within MST.[3] In these off-stoichiometric $Ni_{50}Mn_{50-x}Sn_x$ Heusler alloys, those Mn atoms that exceed the stoichiometric composition (i.e., Ni_2MnSn) occupy a fraction of the Ni or Sn sites in the crystal structure and couple antiferromagnetically to the surrounding Mn atoms at regular Mn sites.[1,4] Hence, this leads to the coexistence of both types of magnetic exchange interactions between Mn atoms within MST. A further manifestation of the latter is the occurrence of the exchange bias (EB) phenomenon that is a distinct feature of martensite in these materials that is typically observed below 100 K.[24–26] It is noteworthy that the major magnetic transition at 195 K is no longer discernible in the heating/cooling *M(T)* curves measured at 50 kOe [Fig. 2(a)]. This thermomagnetic behavior suggests that the alloy undergoes an intermartensitic phase transition upon cooling. To prove this hypothesis, two additional measurements were carried out: (1) the heating and cooling of DSC curves above room temperature to determine the phase transformation behavior of the 10M monoclinic MST, and (2) the measurement of the magnetization hysteresis loops of the sample after FC under $H = 20$ kOe, in the temperature range of 100 and 4 K to check if the EB effect exists in the sample. The fact that the intermartensitic transition vanishes at high magnetic fields ($H = 50$ kOe) suggests that structural modification induced by the intermartensitic transition has a minimal effect on the magnetic structure of the system.

Figure 2(b) shows the DSC curves over the temperature range of 265–370 K. The well-defined endothermic/exothermic peaks above room temperature during the heating and cooling cycles in the heat flow DSC curves confirm the occurrence of the first-order martensite-to-austenite phase transition. Starting and finishing structural transition temperatures of $A_S = 321$ K and $A_f = 330$ K, $M_S = 321$ K and $M_f = 312$ K have been estimated by simple extrapolation from the curves. The transformation exhibits a thermal hysteresis of 9 K (determined as $\Delta T = A_f - M_S$). Hence, a weakly magnetic or paramagnetic 10M monoclinic martensite transforms into a paramagnetic AST. Similar values of A_S, A_f, M_S, M_f, and ΔT can be obtained from the *M(T)* curve measured

at 50 kOe (shown in the inset of Fig. 2(b)). The magnetic transition temperatures, determined from both methods, are summarized in Table I and are in excellent agreement. The crystal structure of the high temperature MST, as well as the structural and magnetic transitions temperatures determined for $Ni_{51.2}Mn_{36.8}Sn_{12.0}$ ribbons, differ from that reported for bulk polycrystalline alloys, specifically for the alloy $Ni_{50}Mn_{40}Sn_{10}$, which has a similar e/a ratio of 8.18.[3] According to Ref. 3, MST has a 14M monoclinic crystal structure with a broad magnetic transition at 137 K, and with characteristic temperatures for the reverse and direct MT of $A_S = 445$ K, $A_f = 453$ K, $M_S = 444$ K, and $M_f = 437$ K ($\Delta T = 10$ K).

Measurement of magnetization hysteresis loops from the thermally demagnetized state in the temperature range from 4 K to 300 K reveals that the alloy shows a dominant FM behavior across the whole temperature range. However, if the sample is cooled from 150 K to selected temperatures below ~100 K under a 20 kOe magnetic field and the FC magnetization hysteresis loops are subsequently measured from 20 kOe to −20 kOe for a complete cycle, the loops progressively shift along the negative H-axis, indicating that EB exists in the sample. EB and coercive field are given by $H_E = -(H_1 + H_2)/2$, and $H_C = |(H_1 - H_2)|/2$, respectively, where H_1 and H_2 are the left and right field values of the applied field at which the magnetization equals zero. Fig. 3(a) shows the low-field region of FC hysteretic loops (i.e., -2500 Oe $\leq H \leq +2500$ Oe) at 5 and 100 K. The field shift disappears at ~100 K (and the loops are symmetric for $T \geq 100$ K). As Fig. 3(b) shows, the H_E continuously decreases with increasing temperature and vanishes at this temperature, which can be defined as the blocking temperature T_B of the system. As previously reported,[24–26] the exchange bias is a characteristic phenomenon of MST in these off-stoichiometric alloys that is very sensitive to the Mn content.[25,26] It is attributed to the unidirectional magnetic anisotropy produced by the exchange coupling of AFM and FM components when the system is FC from a temperature above T_B. The temperature dependence of H_C from 4 to 300 K is represented in Fig. 3(b). As the temperature increases, H_C rises and peaks at 1017 Oe at around 50 K. Above 50 K, H_C progressively decreases approaching zero close to 195 K. But above this temperature, H_C increases again to 20 Oe to become zero close to 308 K. The very different coercivity values measured in both temperature intervals suggest a notable difference in the magnetocrystalline anisotropy of both martensites (i.e., the low-temperature MST shows higher magnetocrystalline anisotropy than the one existing above 195 K).

In summary, from the present study, we conclude that: (a) rapidly solidified ribbons of the Heusler alloy $Ni_{51.2}Mn_{36.8}Sn_{12.0}$ crystallize as a single-phase magnetic MST that at RT shows a 10-layered modulated monoclinic structure that has a magnetic transition at 308 K. DSC and magnetization studies confirm that in the paramagnetic region this phase transforms martensitically. (b) The major magnetic transition observed around 195 K upon cooling has been ascribed to an intermartensitic phase transformation. (c) The observation of an EB effect below 100 K and the behavior of low-field $M(T)$ curves below 195 K demonstrate that the existing phase below this temperature is also MST and (d) that the different behavior shown by the temperature dependence of the coercive field suggests that the low-temperature MST has higher magnetocrystalline anisotropy than the high-temperature MST.

TABLE I. Phase transition temperatures and thermal hysteresis (defined as $\Delta T = A_f - M_S$) for the reverse and direct MT determined from the $M(T)^{50\,kOe}$ and DSC curves.

Method	A_S (K)	A_f (K)	M_S (K)	M_f (K)	ΔT (K)
DSC	321	330	321	312	9
$M(T)$ curve	324	331	322	315	9

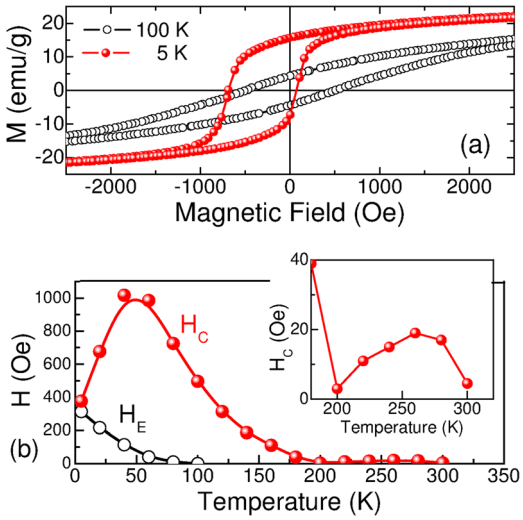

FIG. 3. (a) Low-field region of FC hysteresis loops at 5 K and 100 K. (b) Temperature dependence of the coercive field and EB field. Inset: high magnification of the temperature range of 180–320 K for the $H_C(T)$ curve.

Authors acknowledge the financial support from: (a) CONACYT, Mexico (Projects CB-2010-01-157541 and CB-2012-176705); (b) ICyTDF, UACM, and Gobierno del Distrito Federal-Mexico; (c) LINAN (IPICyT); and Spanish CSIC (C.F.S.V. Ph.D. Grant JAEPRE-08-00508). Technical support of M.Sc. G. J. Labrada- Delgado and M. Onbasli is also recognized.

[1]A. Planes *et al.*, J. Phys.: Condens. Matter **21**, 233201 (2009).
[2]Y. Sutou *et al.*, Appl. Phys. Lett. **85**, 4358 (2004).
[3]T. Krenke *et al.*, Phys. Rev. B **72**, 014412 (2005).
[4]T. Kanomata *et al.*, Mater. Sci. Forum **583**, 119 (2008).
[5]V. V. Martynov and V. V. Kokorin, J. Phys. III France **2**, 739 (1992).
[6]N. Vasilev *et al.*, JETP Lett. **58**, 306 (1993).
[7]Y. C. Lo, S. K. Wu, and H. E. Horng, Acta Metall. Mater. **41**, 747 (1993).
[8]S. H. Chang *et al.*, Mater. Sci. Eng., A **476**, 316 (2008).
[9]H. Kang, S. Wu, and L. Wu, J. Alloys Compd. **509**, 1619 (2011).
[10]T. Inoue *et al.*, Mater. Lett. **19**, 33 (1994).
[11]S. Morito and K. Otsuka, Mater. Sci. Eng., A **208**, 47 (1996).
[12]V. A. Chernenko *et al.*, Acta Mater. **50**, 53 (2002).
[13]W. H. Wang *et al.*, Phys. Rev. B **66**, 052411 (2002).
[14]C. Segui *et al.*, Acta Mater. **53**, 111 (2005).
[15]V. V. Khovailo *et al.*, J. Phys.: Condens. Matter **16**, 1951 (2004).
[16]S. Chatterjee *et al.*, J. Magn. Magn. Mater. **324**, 1891 (2012).
[17]M. Khan, S. Stadler, and N. Ali, J. Appl. Phys. **99**, 08M705 (2006).
[18]R. F. Hamilton *et al.*, Acta Mater. **55**, 4867 (2007).
[19]S. Y. Yu *et al.*, J. Magn. Magn. Mater. **322**, 2541 (2010).
[20]J. D. Santos *et al.*, J. Appl. Phys. **103**, 07B326 (2008).
[21]B. Hernando *et al.*, J. Magn. Magn. Mater. **321**, 763 (2009).
[22]X. C. Xuan *et al.*, Appl. Phys. Lett. **92**, 242506 (2008).
[23]D. L. Schlagel *et al.*, Scr. Mater. **59**, 1083 (2008).
[24]Z. Li, C. Jing *et al.*, Appl. Phys Lett. **91**, 112505 (2007).
[25]M. Khan *et al.*, J. Appl. Phys. **102**, 113914 (2007).
[26]S. Esakki *et al.*, J. Appl. Phys. **110**, 023904 (2011).